DOE/PC/70021-3

DIRECT SYNTHESIS OF 2-METHYL-1-PROPANOL/METHANOL FUELS AND FEEDSTOCKS

Quarterly Technical Progress Report for the Period

June - August 1985

DOE/PC/70021--3

DE89 008259

Kamil Klier
Richard G. Herman
Gary W. Simmons

with
John Nunan
Paul B. Himelfarb

Center for Surface and Coatings Research
and
Department of Chemistry
Lehigh University
Bethlehem, PA 18015

September 1985

PREPARED FOR THE UNITED STATES
DEPARTMENT OF ENERGY

Under Contract No. DE-AC22-84PC70021

DIRECT SYNTHESIS OF 2-METHYL-1-PROPANOL/METHANOL FUELS AND FEEDSTOCKS

DIRECT SYNTHESIS OF 2-METHYL-1-PROPANOL/METHANOL FUELS AND FEEDSTOCKS

OBJECTIVES AND SCOPE OF WORK

The objective of this research project is to provide a technological and scientific foundation for the synthesis of 2-methyl-1-propanol/methanol fuels and basic chemicals from synthesis gas. These mixtures are excellent high octane fuels, can be blended with hydrocarbon gasoline, have high energy densities in the 2-methyl-1-propanol portion, and have synthesis stoichiometries that can be adjusted to the various H_2/CO ratios produced by different gasifiers and feedstocks.

The two principal tasks involve the following lines of research:

(i) the development and optimization of Cs/Cu/ZnO support catalysts wherein the cesium component provides a very effective basic function that steers the synthesis toward 2-methyl-1-propanol, and

(ii) the development of a kinetic reaction network that will be usable for reactor design, as well as for predictions of reaction conditions that give rise to the required 2-methyl-1-propanol/methanol composition in the reactor exit stream.

Auxiliary tasks of this research project that will utilize and build upon the data and principles derived from the two primary tasks deal with

(iii) providing mechanistic input into the kinetic modelling scheme based on experimental research using chemical trapping of surface intermediates, isotopic studies, and insitu infrared spectroscopy,

(iv) exploratory research into novel basic components, consisting of aluminosilicates and amines, that promote branching during carbon-carbon bond formation, and

(v) concurrent characterization of the catalysts by gaseous chemisorption techniques and by utilizing the modern techniques of HR-TEM, STEM, electron and X-ray diffraction, X-ray photoelectron spectroscopy, and vibrational spectroscopies such as laser Raman microprobe spectroscopy.

SUMMARY OF PROGRESS

Last quarter, the promotional effect of cesium doping of the binary 30/70 Cu/ZnO catalyst on the synthesis of methanol and higher alcohols was studied in detail. During the present quarter, an intensive series of aluminum-supported catalysts, both Cs promoted and unpromoted, have been prepared by a special preparation technique and tested to determine alcohol synthesis activity, selectivities, and stability. Preparation of a single-phase hydrotalcite-like $[Cu_xZn_{1-x})_6Al_2CO_3(OH)_{16}\cdot 4H_2O]$ catalyst precursor has been successfully accomplished. TEM studies show that both the precursor and the oxide form that is produced by calcination exist in a single platelet morphology. X-Ray powder diffraction surprisingly demonstrates that rehydration of the calcined oxide form of the ternary catalyst, e.g. during pelletization from an aqueous slurry, leads to reconstitution of the hydrotalcite-like structure.

Some of these catalysts have been tested to determine their activities in producing methanol and higher alcohols. Some of the others will be tested in the near future. Since testing for (i) methanol and for (ii) higher alcohols is carried out at different temperatures and H_2/CO ratios, the methanol yield is sometimes used as an indicator of the probable yield of higher alcohols if other reaction parameters, e.g. GHSV, are maintained. It has been observed that catalysts obtained by calcination and reduction of the hydrotalcite-like precursor are very active methanol synthesis catalysts. Doping these catalysts

with cesium in an aqueous solution leads to initial deactivation, which is partially recovered by doping at higher cesium levels. Initial studies show that catalysts derived from mixed phase precursors (hydrotalcite and aurichalcite) or pure phase hydrotalcite exhibit low selectivity for higher alcohol synthesis while still being active methanol synthesis catalysts. However, these ternary catalysts have a low bulk density so that a fairly high GHSV based on catalyst weight (l/kg catalyst/hr) was utilized. A lower GHSV should enhance the yield of higher alcohols. While deactivation of cesium-promoted binary Cu/ZnO catalysts was minimal, doping of the ternary catalysts with cesium led to some gradual deactivation upon prolonged testing, as already noted, but a marked increase in catalyst stability under higher alcohol synthesis conditions was produced by higher loading levels of cesium in the ternary catalyst. The experimental results obtained during this quarter give us guidelines for altering the promoter doping procedure so that a more active and selective aluminum-supported higher alcohol synthesis catalyst will be obtained.

TECHNICAL PROGRESS

Preparation and Testing of Cu/Zn/Al Catalysts

Introduction

The object of the work described in this report is the preparation and testing of Cu/Zn/Al catalysts that are being developed for the selective synthesis of higher alcohols. The work carried out is divided into the following parts:

(i) Preparation of the single morphology Cu/Zn/Al catalyst precursor having a hydrotalcite-like structure. Note that hydrotalcite is a naturally occurring mineral having the typical composition of $Mg_6Al_2(OH)_{16}CO_3 \cdot 4H_2O$, whereas the catalyst precursor prepared here has (Cu,Zn) in place of the Mg and is isomorphous with the natural mineral. Thus, the (Cu,Zn)-containing compound is referred to in this report as the hydrotalcite-like, or even the hydrotalcite, precursor.

(ii) Testing of the Cu/Zn/Al catalyst after calcination and reduction of the hydrotalcite-like precursor, both under methanol and higher alcohol synthesis conditions.

(iii) Doping of the Cu/Zn/Al catalyst with cesium, followed by testing under both methanol and higher alcohol synthesis conditions; where several doping procedures were examined.

(iv) Determining the long-term stability of the cesium doped and undoped catalysts.

(v) Comparison of the activities of catalysts derived from the pure phases of hydrotalcite and aurichalcite with those obtained with catalysts derived from mixed phases of hydrotalcite and aurichalcite.

Catalyst Preparation

Preparation of the hydrotalcite precursor involved the systematic variation of a number of variables in the coprecipitation process. These included pH, temperature, presence or absence of sodium acetate in the reaction mixture, and aging time. The chemical composition of the salt solution used was kept within certain limits because of the unique structure of the hydrotalcite-like precursor that was to be formed. The chemical composition of hydrotalcite can be varied over a given range as determined by the following criteria:

$$HC = (Cu_xZn_{1-x})_6Al_2CO_3(OH)_{16}\cdot 4H_2O$$

$$0 \leq \frac{Cu}{Cu+Zn} \leq 0.5;\ 0.24 \leq \frac{Al}{Al+M^{n+}} \leq 0.31$$

The molar ratio of the metal ions used in the initial preparations were Cu:Zn:Al = 30:45:25. The apparatus used in the preparations is shown in Figure 1, and consists of a constant temperature water bath, two high precision liquid pumps that deliver the metal salt solution and the Na_2CO_3 solution separately to the reaction vessel, a digital pH meter accurate to $\pm$ 0.01 pH units, and a stirrer.

The same general method was used for all the hydrotalcite preparations except for variations in such reaction conditions as pH, precipitation procedure, presence or absence of sodium acetate and aging time of the precipitate. A list of all samples prepared and the conditions used are given in Table 1. A detailed description of the preparation of only one sample, HC-17, is given since this sample was extensively used in catalyst

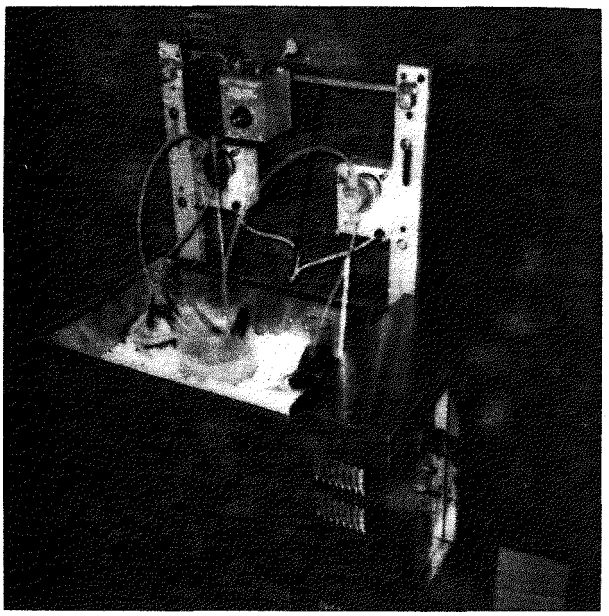

Figure 1. Apparatus used in the preparation of Cu/Zn/Al hydrotalcite-like precursors

TABLE 1

Preparation conditions and purity of the different Hydrotalcite-like precursors. Hydrotalcite purity is taken as the ratio of XRD intensity of the major Hydrotalcite peak at 11.8°(2θ) to the major impurity peak at 19.6°(2θ).

HC #	pH	Sodium Acetate Present	Temp.(°C)	Aging Time (minutes)	Purity $\frac{I_H}{I_H+I_i}$
HC-2	8.0	No	65	10	0
HC-3	6.5	No	80	10	0
HC-4	5.75-8.8	No	82	10	0.63
HC-5	5.8 - 8.8	No	60	10	0.84
HC-6	6.5	Yes	60	10	0
HC-7	7.0	Yes	60	10	0.80
HC-8	7.5	Yes	60	10	0.53
HC-9	8.0	Yes	60	10	0.86
HC-10	8.5	Yes	60	10	0.94
HC-11	9.0	Yes	60	10	0.98
HC-12	8.0	No	60	10	0.82
HC-13(i)	9.5	Yes	60	5	1.0
HC-13(ii)	9.5	Yes	60	30	1.0
HC-14	9.0	Yes	60	10	0.98
HC-15	9.0	Yes	40	10	0.98
HC-16	9.0	Yes	50	10	0.98
HC-17	9.5	Yes	50	30	1.0
HC-18	9.5	Yes	50	30	1.0
HC-19	9.5	Yes	50	30	1.0
HC-20	9.65-10.94	No	50	30	1.0
HC & AU	6.5	Yes	60	30	0.96

testing. The procedure used for the preparation of HC-17 utilized the following reagents: (i) salt solution consisting of 0.3M $Cu(NO_3)_2 \cdot 2\frac{1}{2}H_2O$, 0.45M $Zn(NO_3)_2 \cdot 6H_2O$ and 0.25M $Al(NO_3)_3 \cdot 9H_2O$; (ii) 1M Na_2CO_3; and (iii) 1000 ml of 1M sodium acetate. Both the metal salt solution and Na_2CO_3 solution were stored in 1000 ml erlenmeyer flasks and placed in the constant temperature bath. The reaction vessel consisted of a 3000 ml beaker containing initially 1000 ml of 1M sodium acetate. The bath temperature was adjusted such that the reaction vessel temperature of exactly 50°C was achieved while the solution was stirred at a constant rate of 220 revolutions per minute. After equilibration for 60 min, the pH of the sodium acetate solution was noted (≈8.3) and the pH adjusted to 9.5 by controlled addition of 1M Na_2CO_3. After allowing the solution to equilibrate for 5 min, both the salt solution and Na_2CO_3 were fed into the reaction vessel. The salt solution pump was set to deliver 2.82 ml/min and the Na_2CO_3 solution feed rate was adjusted as to keep the pH constant at 9.5. It was found that the required feed rate of the Na_2CO_3 solution varied with time, as shown in Table 2.

After 120 min both the salt addition and Na_2CO_3 addition were stopped and the precipitate allowed to digest for 30 min while maintaining continuous stirring. The reaction vessel was then removed from the constant temperature bath, and the precipitate was allowed to settle for 20 min. For the particular case of HC-17, the precipitate was found to be very fine and did not settle readily. About 70% of the supernatent solution was then decanted and 1000 ml of warm distilled water (≈50°C) was added to the precipitate. The precipitate was subsequently filtered using a Buckner funnel and washed

TABLE 2

Feed rate of 1M Na_2CO_3 as a function of time needed to keep pH at 9.5 in the preparation of HC-17

Time (Min)	pH	Na_2CO_3 feed rate (ml/min)
0	9.5	9.27
	pH is decreasing rapidly	
5.0	9.45	13.0
10.0	9.5	16.5
	pH has stabilized	
15.0	9.45	16.5
20.0	9.5	17.1
30.0	9.51	17.8
40.0	9.49	17.0
50.0	9.5	17.6
60.0	9.5	17.6
70.0	9.5	17.6
80.0	9.5	17.6
90.0	9.5	17.6
100.0	9.5	17.6
110.0	9.5	17.8
120.0	9.5	17.8

with 700 ml of warm distilled water (≈50°C). After air filtering for 10 min, the semi-solid precipitate was placed into 2000 ml of warm distilled water, which was then stirred vigorously for 5 min. After settling for 15 min, the water was decanted and the solid was filtered again using a Buckner funnel. After additional air filtering for 10 min, the above washing procedure was repeated. The precipitate was finally air filtered for 20 min and allowed to air dry at ambient temperature for several days. The yield of HC-17 precursor was found to be ≈49 g.

In the preparation of HC-19 the salt solution consisted of 0.3M $Zn(NO_3)_2 \cdot 6H_2O$, 0.45M $Cu(NO_3)_2 \cdot 2H_2O$ and 0.25M $Al(NO_3)_3 \cdot 9H_2O$. Otherwise, the procedure was the same as for HC-17. HC-20 was prepared by addition of the salt solution (Cu:Zn:Al = 30:45:25) to 1000 ml of 1M Na_2CO_3 at 50°C using a feed rate of 2.82 ml/min for 90 min. The pH was monitored as a function of time and found to decrease from 10.94 at zero time to 9.65 after 90 min. HC-18, HC-19 and HC-20 will be tested in the near future.

Chemical analysis using atomic absorption for Na, Cu, Zn and Al was carried out on the precursors HC-17, HC-18, HC-19 and HC-20, and the results are presented in Table 3. The wt% of Na is shown and the metals are presented as molar ratios. It is evident that the washing procedure used to remove Na has been very effective and that the metal molar ratios are close to the nominal elemental concentration ratios utilized in the reactants.

Precursor Characterization

After the preparation of each hydrotalcite sample, the purity was determined by X-ray powder diffraction (XRD). A reference XRD pattern for Cu,Zn

TABLE 3

Chemical analysis of HC-17, HC-18, HC-19 and HC-20

HC-#	Theoretical Molar Ratio Cu:Zn:Al	Experimental Molar Ratio Cu:Zn:Al	Weight % Na
HC-17	30:45:25	29.7:45.8:24.5	0.014
HC-18	30:45:25	30.0:46.0:24.0	0.026
HC-19	45:30:25	43.0:31.5:25.5	0.009
HC-20	30:45:25	27.7:47.3:25.0	0.011

hydrotalcite was taken from Busetto et al. (1), and is shown in Figure 2g. This figure also shows that pH had a dramatic effect on the purity of the end product. Coprecipitation at pH = 6.5 gave only aurichalcite. Upon increasing the pH, the percentage of hydrotalcite in the product increased rapidly until above pH = 9.0, where the precipitate consisted only of hydrotalcite. (This is evident by comparing Figure 2f (HC-17) and 2g, and the corresponding d-spacings presented in Table 4). In addition, the overall yield of precipitate was found to increase with increasing pH. The effect of temperature and the presence of sodium acetate during co-precipitation are shown in Figures 3 and 4, respectively. Temperature was found to have little effect in the range studied except for slightly increased yield in going from T = 60°C to T = 40°C. From Figure 4 it is noted that the presence of sodium acetate gave rise to a purer hydrotalcite preparation. Aging of the precipitate for different time periods did not greatly effect the end product, as shown in Figure 5.

Catalyst Pretreatment

Before testing or doping, the precursor was pelletized and sieved to particle sizes ranging from 0.85 to 2.0 mm in dimension. The catalyst was then calcined by heating in air to 100, 150, 200, 250, 300°C for 0.5 hr each, and finally to 350°C for 3.0 hr. This procedure converted the precursors from the hydroxycarbonate form to the oxide form. After cooling, the catalyst was loaded into the reactor and reduced in 2% H_2/N_2 at 250°C or alternatively doped with cesium. Doping was carried out by adding the catalyst to 25 ml of an aqueous solution of CsOOCH, followed by evaporation to dryness under

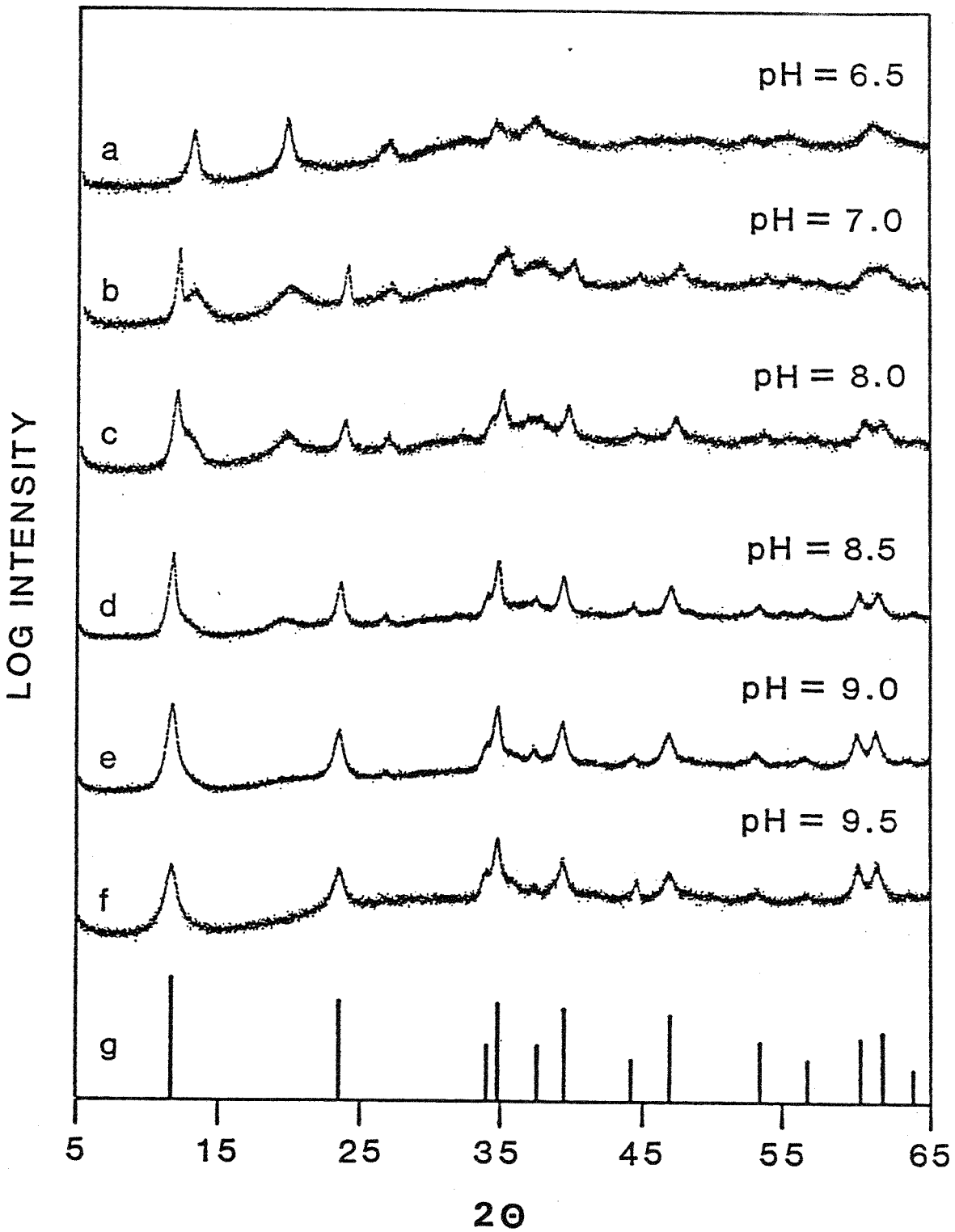

Figure 2. X-Ray diffraction powder patterns showing the effect of pH on Cu/Zn/Al hydrotalcite purity. Preparation conditions were: T = 60°C, aging time = 10 min, coprecipitated in the presence of sodium acetate at pH of a) 6.5 (HC-6), b) 7.0 (HC-7), c) 8.0 (HC-9), d) 8.5 (HC-10), e) 9.0 (HC-11), and f) 9.5 (HC-13) with 5 min aging time). Reference spectrum g is that from Busetto et al. (1).

TABLE 4

X-Ray Powder Diffraction Data for HC-17 and Reference Hydrotalcite

HC-17		$Cu_2Zn_4Al_2(OH)_{16}CO_3 \cdot 4H_2O$ [a]		
d(Å)	I/I_o	d(Å)	I/I_o	hkl
7.484	100	7.540	100	003
3.777	64	3.770	43	006
2.651	24	2.642	8	101
2.593	98	2.589	41	012
2.410	11	2.407	9	104
2.300	58	2.293	35	015
2.052	13	2.054	5	107
1.942	44	1.937	29	018
1.727	18	1.723	10	10$\underline{10}$
1.631	14	1.627	5	01$\underline{11}$
1.540	37	1.536	12	110
1.509	40	1.505	15	113
1.460	12	1.456	4	10$\underline{13}$

[a] Reference data are the calculated lattice parameters taken from Busetto et al. (1).

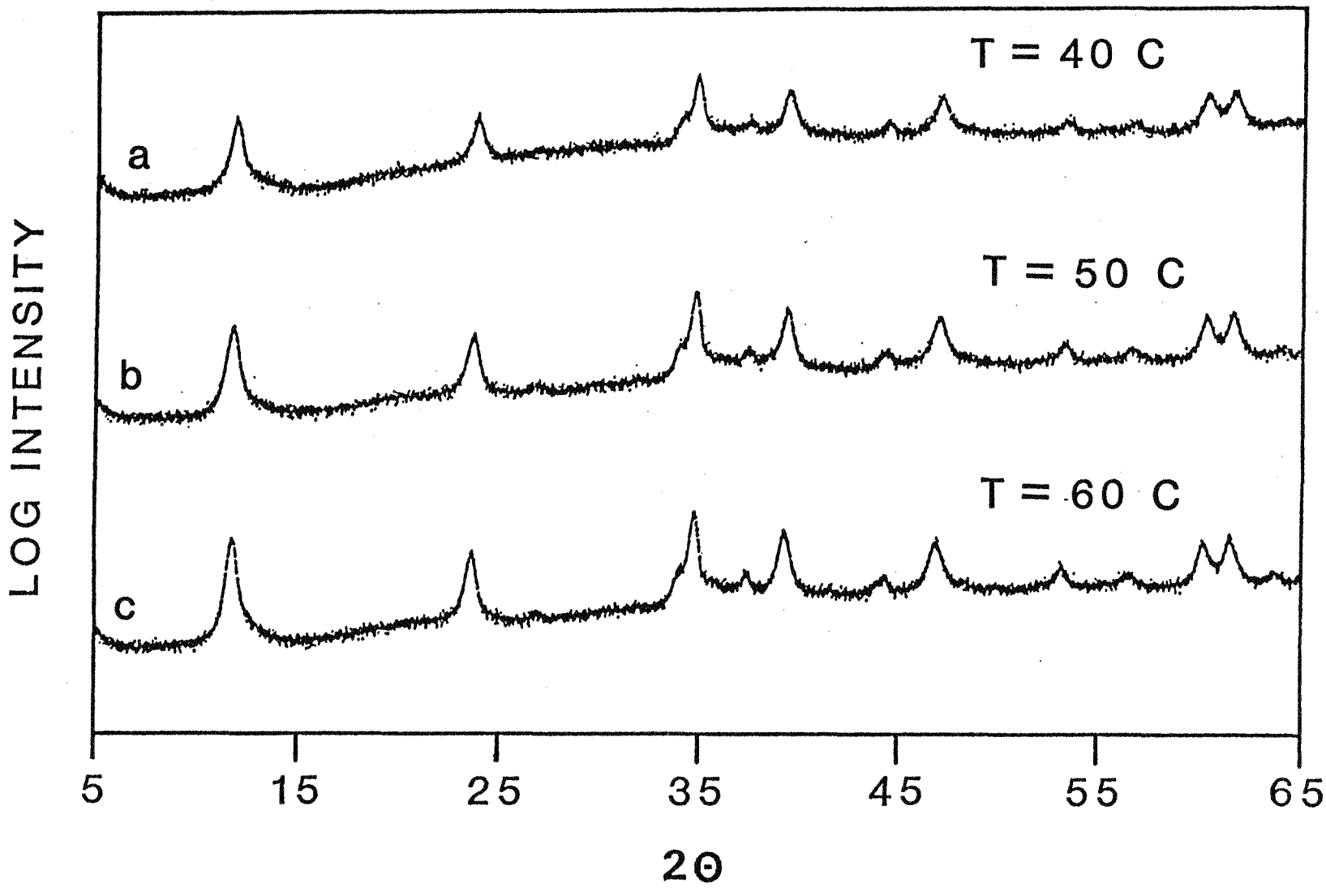

Figure 3. X-Ray diffraction powder patterns showing the effect of coprecipitation temperature on Cu/Zn/Al hydrotalcite purity. Preparation conditions were: pH = 9.0, aging time = 10 min, coprecipitated in the presence of sodium acetate, and temperature of a) 40°C (HC-15), b) 50°C (HC-16), and c) 60°C (HC-14).

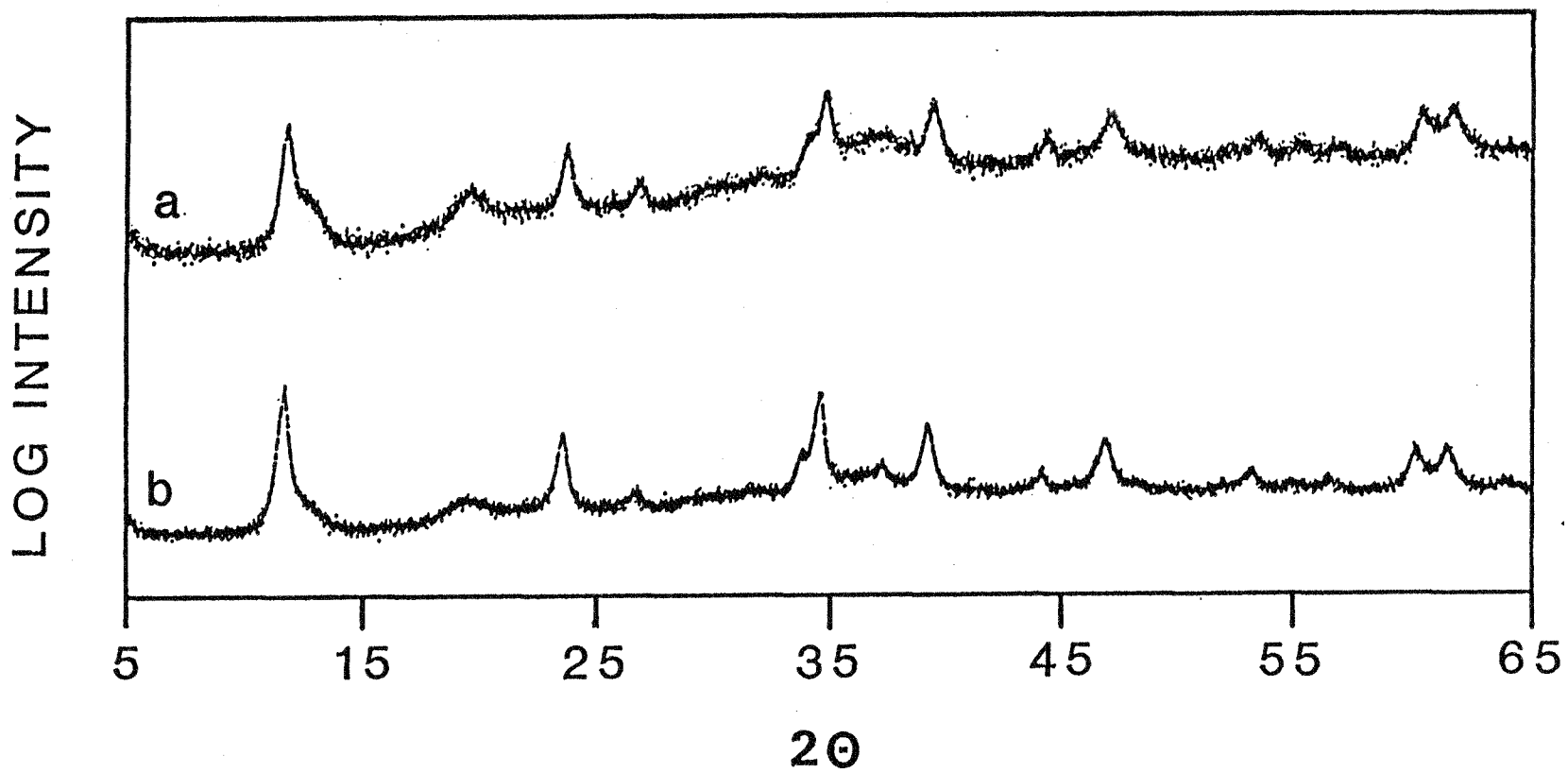

Figure 4. X-Ray diffraction powder patterns showing the effect of coprecipitation in the presence of sodium acetate on Cu/Zn/Al hydrotalcite purity. The major impurity peaks are located at 2θ = 12.9° and 19.6°. Preparation conditions were: T = 60°C, pH = 8.0, aging time = 10 min, and a) without sodium acetate and b) with sodium acetate.

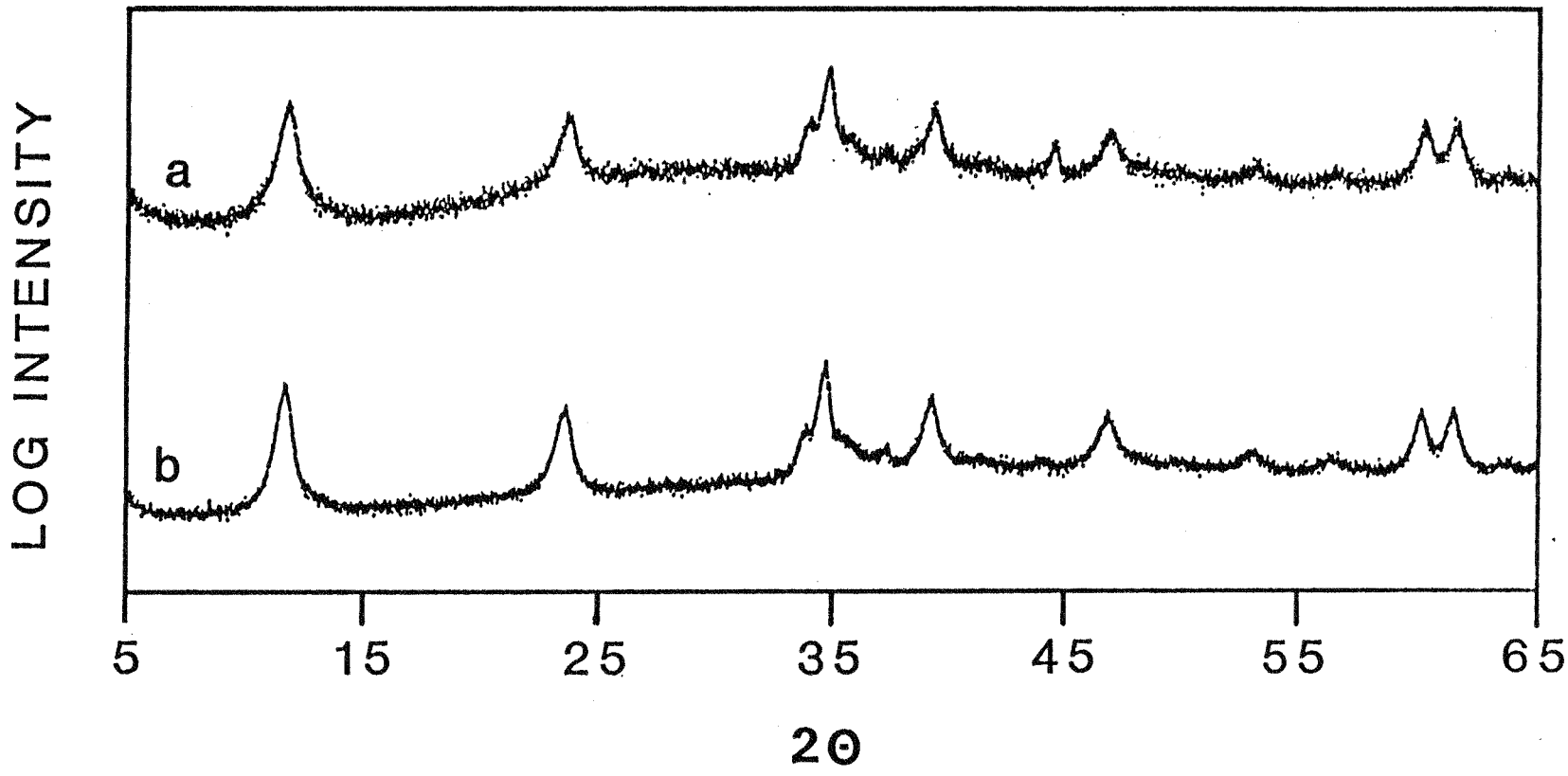

Figure 5. X-Ray diffraction powder patterns showing the effect of aging time after coprecipitation on Cu/Zn/Al hydrotalcite purity. Preparation conditions were: T = 60°C, pH = 9.5, coprecipitated in the presence of sodium acetate and a) aging time = 30 min (HC-13ii) and b) aging time = 5 min (HC-13i).

flowing N_2. After doping, the catalyst was recalcined as described above and loaded into the catalytic reactor for reduction. Reduction was considered to begin at 210°C and the reduction time was calculated based on the amount of H_2 needed to reduce Cu^{2+} to Cu^{o}.

The effect of calcination on the XRD pattern of the HC-17 sample is shown in Figure 6b. It is noted that calcination of the sample led to a nearly featureless XRD spectrum with only a broad peak centered at $2\theta = 36°$. Rehydration of the calcined catalyst, as occurs in Cs doping, gave the hydrotalcite pattern as shown in Figure 6c. However, the peaks are sharper, indicating that reformation of the hydrotalcite structure occurred with an increase in crystallite size when compared to the crystallite sizes for the original precipitate. An increase in particle dimension for the <003>, <015>, <110>, and <113> crystal directions was observed by XRD line broadening as shown in Table 5. This result was confirmed by analysis of the original and reformed hydrotalcite in the transmission electron microscope (TEM). Representative bright field images and corresponding convergent beam diffraction (CBD) patterns are given in Figure 7a-d. An increase in particle size was visably apparent after reformation. The CBD patterns show that the hydrotalcite platelet surface is parallel to the (0001) plane, and that each platelet is a single phase hydrotalcite. It is noted that the particle sizes determined by XRD line broadening are smaller than those observed in the TEM. Evidently, the hydrotalcite crystals have non-uniform strain which adds to the broadening of the XRD peaks.

Calcination of hydrotalcite led to the broad XRD spectrum (Fig. 6b) indicating non-crystalline phases were present. Analysis of the calcined

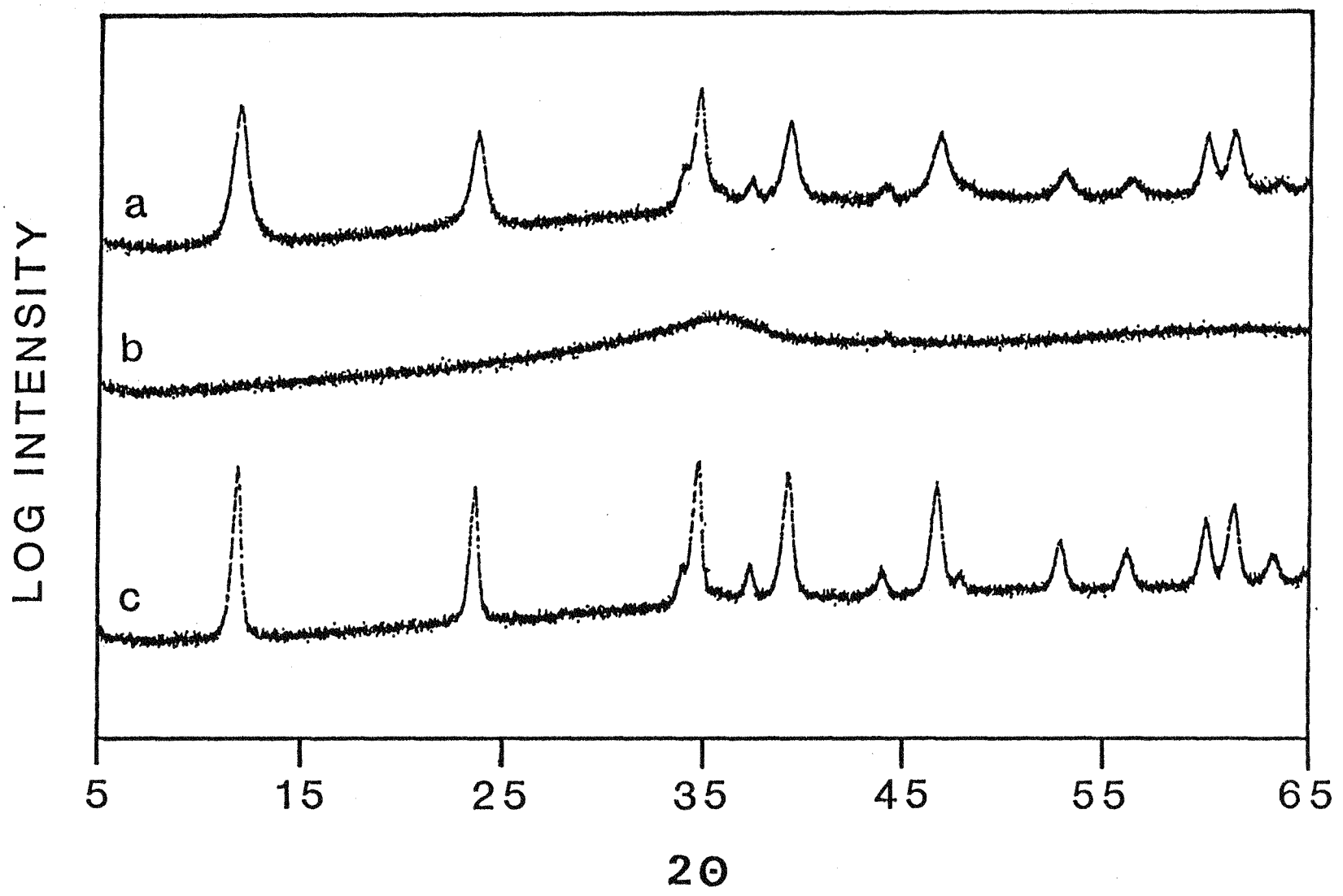

Figure 6. X-Ray diffraction powder patterns showing structural changes accompanying catalyst preparation of HC-17: a) initial Cu/Zn/Al hydrotalcite precursor, b) sample in a), calcined, and c) reformed hydrotalcite after rehydration.

TABLE 5

Particle Dimensions of Hydrotalcite and Recrystallized Hydrotalcite determined by XRD Line Broadening[1]

Crystal Direction	Apparent Dimension (Å)	
	Initial Hydrotalcite	Recrystallized Hydrotalcite
003	135	291
015	153	230
110	200	288
113	181	309

[1] Particle sizes were calculated from the Sherrer equation (2). $d=0.89\lambda/\cos\theta(W_x^2-W_o^2)^{\frac{1}{2}}$, where θ= Bragg angle, W_x the measured peak half-width, W_o the instrumental half-width, and λ the x-ray wavelength of CuK_α radiation, 1.5416 Å.

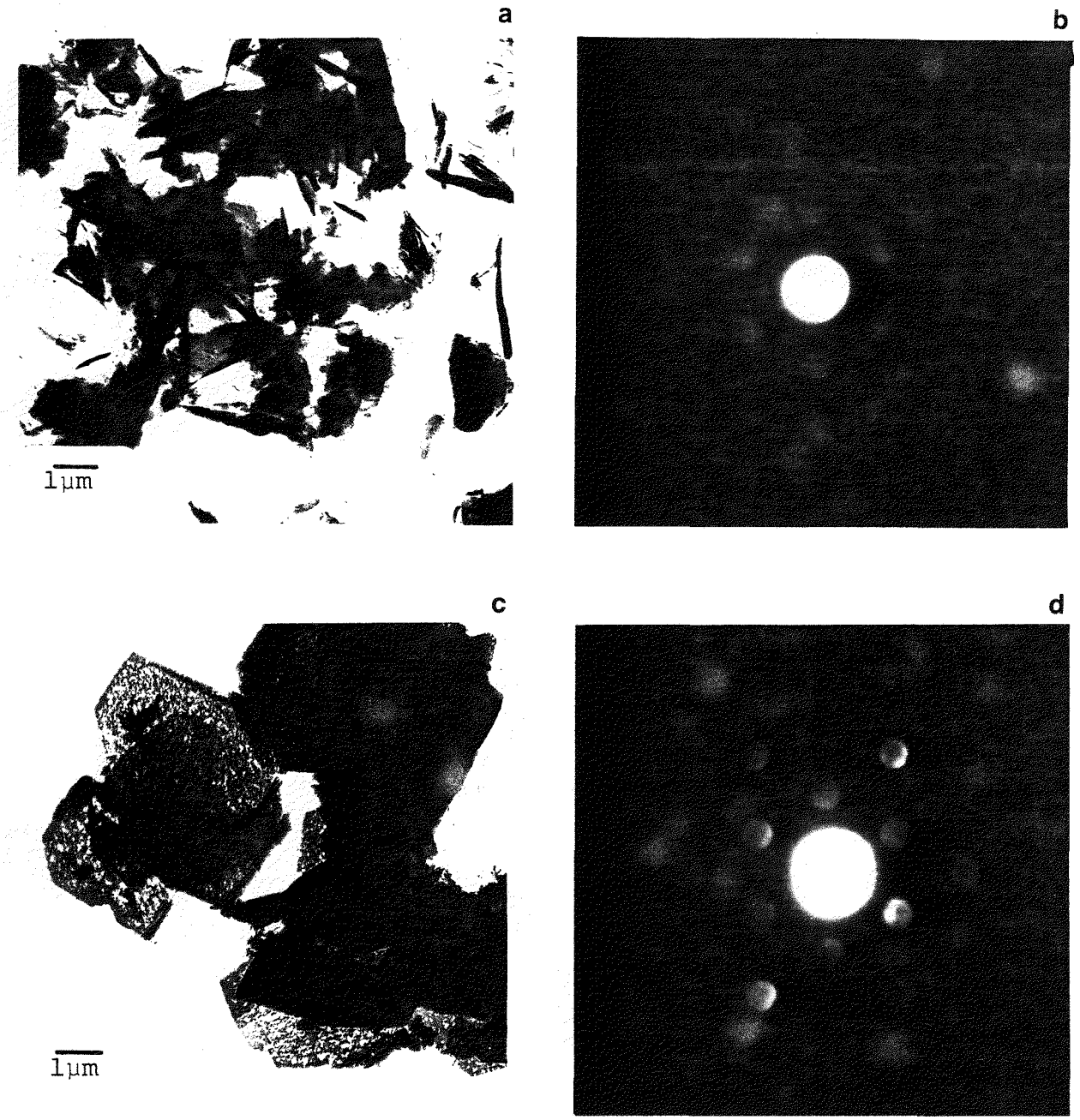

Figure 7. Transmission electron micrographs showing structural and morphological changes accompanying catalyst preparation of HC-17: a) initial Cu/Zn/Al hydrotalcite bright field image (BFI) and b) corresponding convergent beam (40 nm) diffraction (CBD) pattern of (0001) plane, c) BFI of sample in a) calcined and rehydrated and d) corresponding CBD pattern of the hydrotalcite (0001) plane, and e) BFI of sample in c) recalcined and f) corresponding CBD pattern identifying the ZnO (0001) plane.

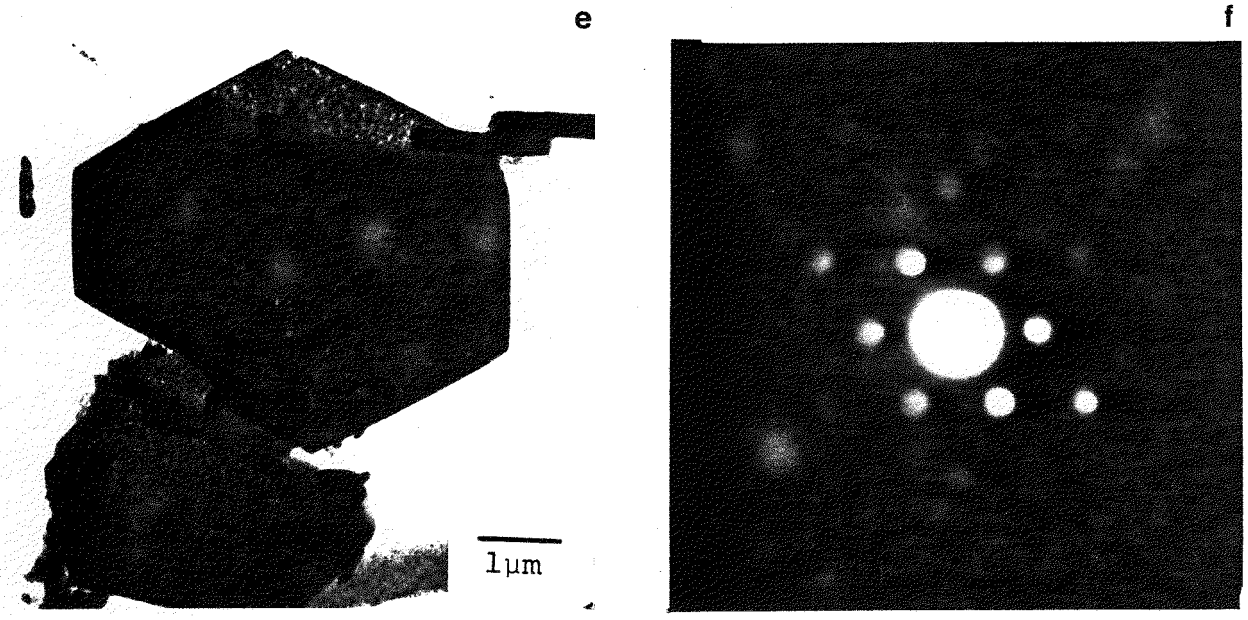

CONTINUATION

Figure 7. Transmission electron micrographs showing structural and morphological changes accompanying catalyst preparation of HC-17: a) initial Cu/Zn/Al hydrotalcite bright field image (BFI) and b) corresponding convergent beam (40 nm) diffraction (CBD) pattern of (0001) plane, c) BFI of sample in a) calcined and rehydrated and d) corresponding CBD pattern of the hydrotalcite (0001) plane, and e) BFI of sample in c) recalcined and f) corresponding CBD pattern identifying the ZnO (0001) plane.

samples in the TEM showed this was the case for the Cu and Al components; however, ZnO was found to be crystalline but with particle sizes less than 3nm. This result was observed in earlier preparations, the results of which have been published (3). The same structural features were observed in the present single phase hydrotalcite preparations, and a platelet and convergent beam diffraction pattern (CBD) due to ZnO from recalcined HC-17 is presented in Figure 7e and 7f. The overall platelet morphology remained after calcination, but the platelets became porous, accounting for the changing structural density.

The activity of the pure hydrotalcite and aurichalcite precursor catalysts were compared with a mixed precursor catalyst previously prepared in this laboratory. The XRD patterns of the original precursor, calcined sample, and reformed hydrotalcite are shown in Figure 8. It is noted that the original precursor consisted mainly of hydrotalcite with a smaller fraction of aurichalcite present. Upon calcination the hydrotalcite and aurichalcite peaks disappeared, and a relatively featureless spectrum with weak peaks centered at $2\theta = 36°$ was produced, indicating the presence of CuO and ZnO. The pretreatment of this sample before activity testing involved initial calcination of the precipitate at 350°C followed by pelletization, which resulted in the formation of single phase hydrotalcite (Figure 8c), after which the catalyst was recalcined before loading into the reactor or doping with cesium.

Catalytic Testing Procedure

Catalysts were tested in such a manner as to obtain the maximum amount of information about catalyst activities and selectivities, and the relationships between catalytic activity and the physical characteristics of the catalysts as determined by surface area measurements, XPS, XRD and TEM studies.

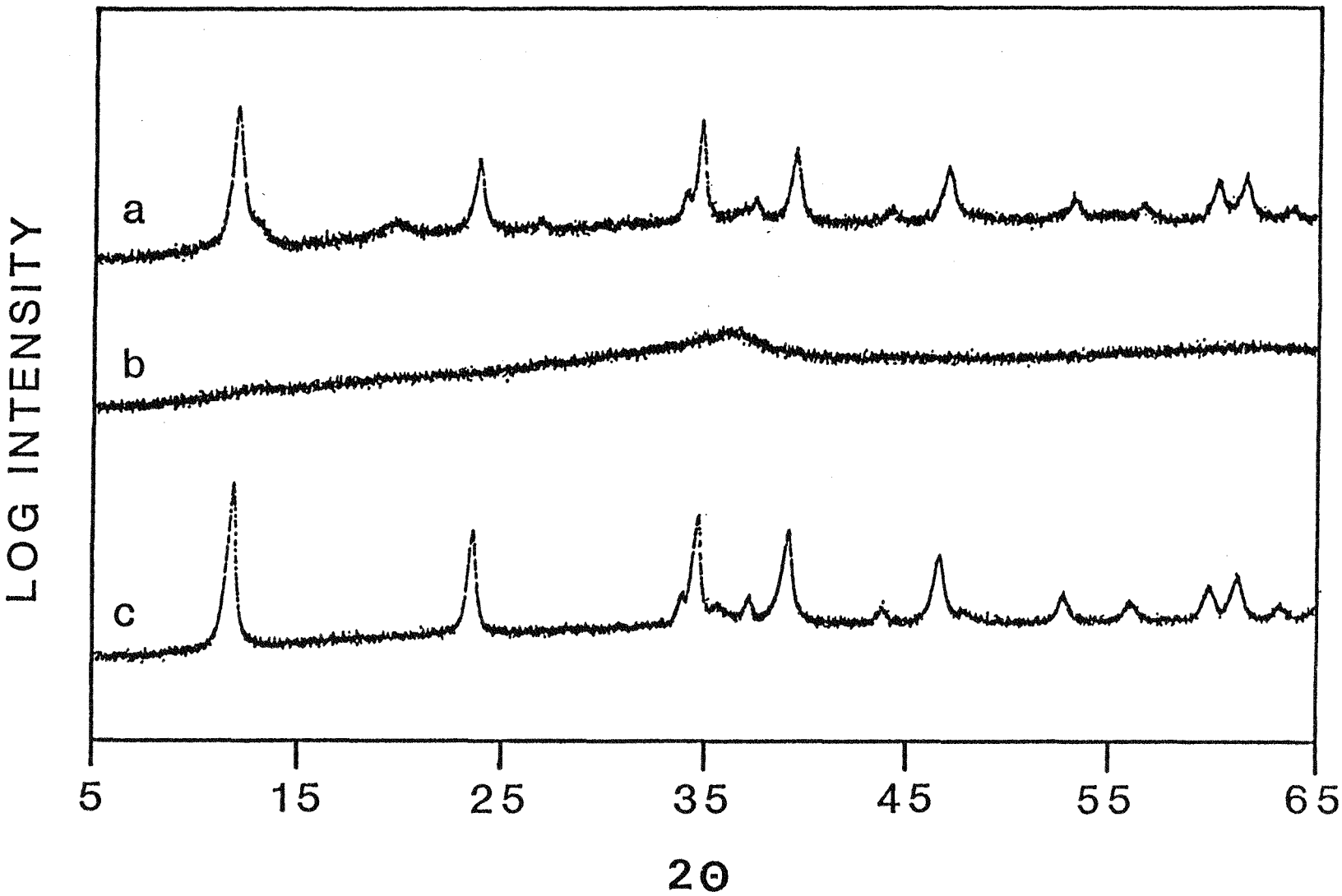

Figure 8. X-Ray diffraction powder patterns showing structural changes accompanying catalyst preparations of sample "HC and AU" (as described in Table 1): a) initial Cu/Zn/Al hydrotalcite/aurichalcite mixed precursor, b) sample in a) calcined and c) reformed single phase hydrotalcite after rehydration.

The testing procedure used to accomplish this was as follows:

(i) Catalyst activities were initially determined under methanol synthesis conditions. This allowed an initial comparison of catalytic activities of the newly synthesized catalysts with the activities of the binary Cu/ZnO samples, both cesium doped and undoped, which were previously tested in this laboratory. These catalysts have been extensively characterized using XRD, XPS and TEM.

(ii) The synthesis conditions were then changed to those used in higher alcohol synthesis, i.e. H_2/CO = 0.45, 250°C, 7.6MPa, and reactant gas flow (F) of 8.0 l/hr, which resulted in a GHSV ≃3260 l/kg catalyst/hr when 2.45 g of catalyst was used. This gave an initial measure of the activity of the catalyst for higher alcohol synthesis while the methanol yield was still far from the equilibrium value.

(iii) The reaction temperature was subsequently increased to 310°C and the activities tested over a long period of time of ≃ 150 hr.

(iv) After extensive testing at 310°C, the temperature was lowered to 250°C and the activity allowed to stabilize for 12 hr.

(v) The reaction conditions were finally changed back to those initially used to measure methanol synthesis activity i.e. T = 250°, F = 15.0 l/hr, and H_2/CO = 2.33.

Steps (iv) and (v) were carried out to give a more accurate measure of the overall level of deactivation of the catalysts for alcohol synthesis. Under higher alcohol synthesis conditions, the methanol yield is close to or at the equilibrium value so that substantial catalyst deactivation may occur before the effect is observed on methanol yield and also in higher alcohol yield, as methanol is considered a precursor to their formation. Under the conditions used in steps (iv) and (v) the methanol yield is well below the equilibrium

value [especially for the condition of step (v)], thus allowing a true measure of the catalyst activity to be obtained. After catalyst testing the samples were removed from the reactor under nitrogen and sealed in four separate glass vials under vacuum to prevent rehydration or reoxidation of the samples before characterization.

The reaction conditions used in testing the ternary Cu/Zn/Al catalysts were similar to those described previously for the binary Cu/ZnO catalysts except that for these hydrotalcite precursor samples, 1.5 g (rather than 2.45 g) of catalyst was used. The catalyst weight was reduced for two reasons:

(i) the density of the hydrotalcite-derived samples was found to be very low such that the volume of 2.45 g of sample plus the glass beads used in dilution gave a catalyst bed length longer than the isothermal portion of the reactor, and

(ii) the initial tests of the undoped hydrotalcite-derived sample, i.e. HC-17, gave much higher than expected methanol synthesis activity.

Presentation of Data

The activity results are presented in both graphical and tabular form. The graphs presented are time plots of activity and give an indication of the overall stability of the catalysts as a function of time on stream. The results presented in tabular form give the yield of products for the given catalyst at different stages of the testing sequence. The data are taken in most cases where the activity has reached a steady or semi-steady state value and then averaged over a given time interval, usually 10-12 hr.

The reaction products were analyzed every 0.5, 1.0 or 2.0 hr, depending on the reaction conditions used. For the long activity study at 310°C, the products were analyzed every 2.0 hr.

Methanol Synthesis Activity

In Figure 9, the activity profile of HC-17 is compared with that of the binary Cu/ZnO catalyst as a function of time on stream for methanol synthesis. It is evident that the HC-17 catalyst is a far superior methanol synthesis catalyst. Both activity profiles pass through a sharp maximum with the maximum yield of methanol being 1.835 kg/kg cat/hr for the HC-17, and 0.554 kg/kg cat/hr for the binary Cu/ZnO catalyst. The activity of HC-17 levels off after 10 hr on stream at 0.888 kg/kg cat/hr as compared to 0.261 kg/kg cat/hr for the binary sample; thus, HC-17 is 3.4 times more active. The sharp maximum for both catalysts may be due to promotion by CO_2 (4), the yield of which was found to follow a profile identical to the methanol yield. In Table 6, the steady state activities averaged over a 12 hr period (except the 0.34 mol% Cu/ZnO where a 6 hr period was used) are presented for the range of catalysts tested. Doping the binary catalyst with cesium leads to a promotion of methanol, methyl formate and ethanol, as already established. Similarly, doping the catalyst derived from the mixed precursor (HC + AU) also leads to a dramatic increase in all three products, with the yield of methanol (0.803 kg/kg cat/hr) being higher than the yield observed for the cesium-doped binary catalyst. The maximum yield over the binary catalyst was found to be 0.620 kg/kg cat/hr at 1.0 mol% cesium loading. The activity of the undoped pure phase hydrotalcite was

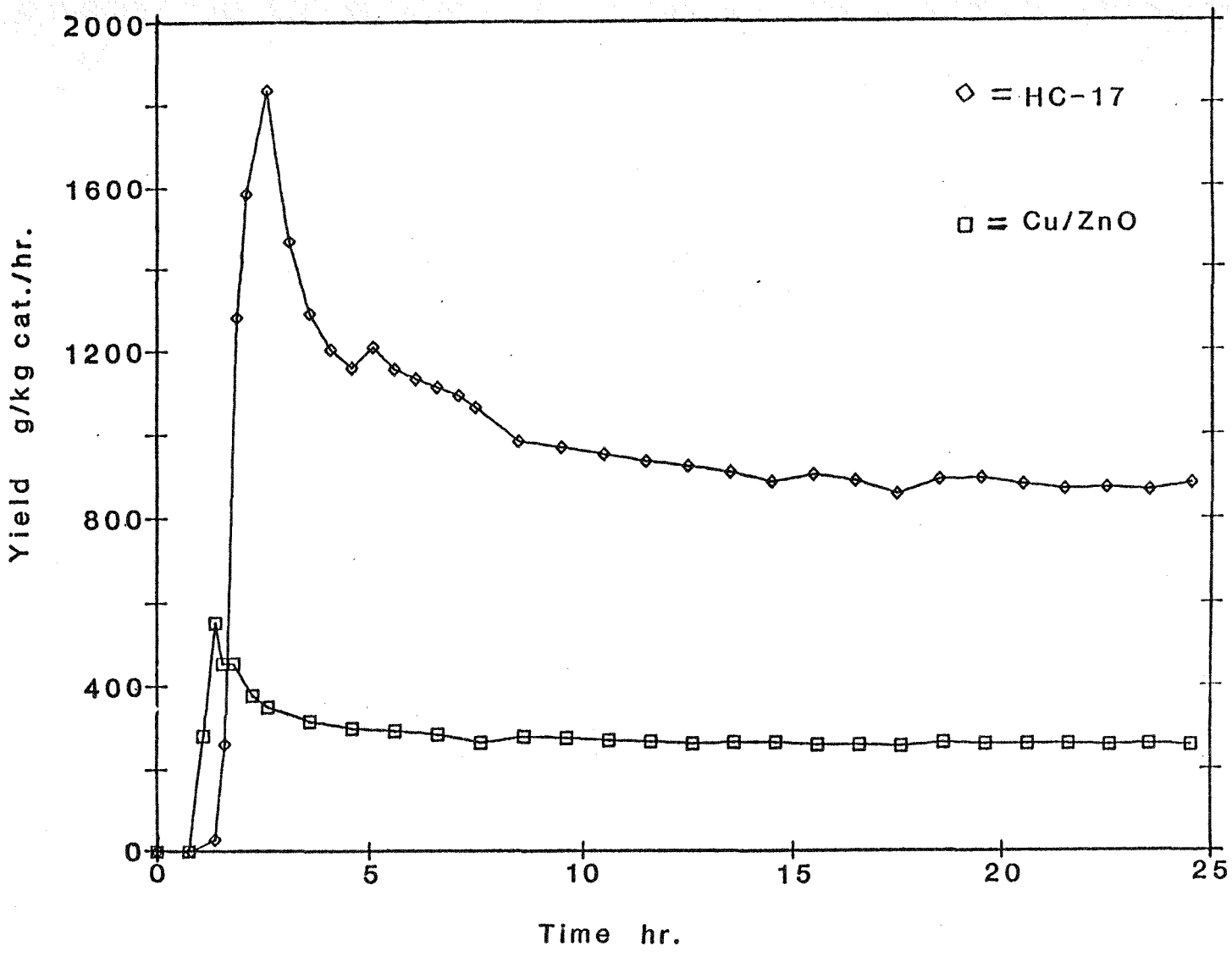

Figure 9. Comparison of the initial activity profile of the binary Cu/ZnO catalyst with that of HC-17 under methanol synthesis conditions. P = 7.6MPa; T = 250°C; Catalyst weight = 2.45 g for the binary catalyst and 1.5 g for HC-17; F = 15 1/hr; H_2/CO = 2.33.

TABLE 6

Comparison of initial activities of catalysts tested, where average activities in the time period shown are presented. P = 7.6 MPa, T = 250°C, F = 15 1/hr and H_2/CO = 2.33. Catalyst weight = 2.45 g for all samples except the HC samples where weight = 1.5 g.

Sample [a]	Time on Stream (hr)	Yield (g/kg cat/hr)					
		CO_2	H_2O	CH_4	CH_3OH	Methyl Formate	C_2H_5OH
AU	12-24	1.2	0.8	-	260.7	1.1	-
AU (doped with 0.34 mol% Cs)	17-23	8.3	0.2	4.3	587.0	5.6	1.0
HC + AU (undoped)	12-24	8.6	0.5	3.0	309.8	0.7	-
HC + AU (doped with 3.0 mol% Cs)	12-24	10.5	0.6	3.9	802.8	3.9	0.6
HC-17 (undoped)	12-24	17.2	1.4	6.5	888.8	-	-
HC-17 (doped with 0.3 mol% Cs	12-24	11.3	1.0	9.4	396.2	-	-
HC-17 (doped with 0.73 mol% Cs)	12-24	15.0	1.0	7.0	699.7	-	-
HC-17 (doped with 2.52 mol% Cs)	12-24	9.5	0.9	5.8	456.2	1.84	-

[a] Sample description given in terms of the precursor structure, AU for aurichalcite and HC for hydrotalcite

found to be even higher at 0.888 kg/kg cat/hr. However, upon doping this sample with 0.3, 0.73 or 2.52 mol% cesium, the activity was surprisingly depressed in marked contrast to the previous results. In Table 7, the effect of changing to higher alcohol synthesis conditions with T = 250°C is shown. In the case of the mixed precursor, the promotion effect of cesium is again evident. However, in the pure hydrotalcite sample doped with increasing levels of cesium, a marked promotion of both methanol and methyl formate was observed, indicating that increasing the loading of cesium led to a recovery of activity initially lost in the doping process. (Undoped HC-17 is currently being tested under higher alcohol synthesis conditions).

Higher Alcohol Synthesis

In Figures 10, 11, 12 and 13, the activity profiles of several of the catalysts are plotted under higher alcohol synthesis conditions where T = 310°C. For the 0.34 mol% cesium doped binary catalyst, little noticeable deactivation was observed for either methanol or higher alcohol synthesis over the 175 hr time period in which the catalyst was tested. However, the mixed precursor catalysts (both doped and undoped) and the doped hydrotalcite samples show some deactivation for higher alcohol synthesis over the same time period. It was further observed that the activity for higher alcohol synthesis was higher over the binary catalyst, whereas the activity for methanol synthesis was lower. The above observations are summarized in Table 8, where the activities in g/kg cat/hr are compared both for the initial activity (2-12 hr on stream) and toward the end of the run (95-107 hr) for all the catalysts tested under these conditions. The times given in the

TABLE 7

Product yield under higher alcohol synthesis conditions of T = 250°C, P = 7.6 MPa, F = 8 l/hr and H_2/CO = 0.45. Catalyst weight = 2.45 g for all samples except HC samples where weight = 1.5 g.

Sample	Time on Stream (hr)	Yield (g/kg cat/hr)							
		CO_2	H_2O	CH_4	CH_3OH	Methyl Formate	C_2H_5OH	Methyl Acetate	C_3H_7OH
AU Doped with 0.34 mol% Cs	26-36	12.8	-	4.0	325.5	14.2	4.3	2.3	2.2
HC + AU Undoped	105-113	10.7	0.3	3.5	220.2	6.2	-	-	-
HC + AU Doped with 3.0 mol% Cs	48-57	11.9	0.1	4.6	293.6	14.6	3.2	0.2	0.6
HC-17 Doped with 0.3 mol% Cs	105-112	11.2	0.3	6.4	207.1	2.8	-	-	-
HC-17 Doped with 0.73 mol% Cs	128-138	11.7	0.1	4.2	254.8	4.6	-	-	-
HC-17 Doped with 2.52 mol% Cs	107-117	12.8	0.7	8.5	445.7	15.8	-	-	-

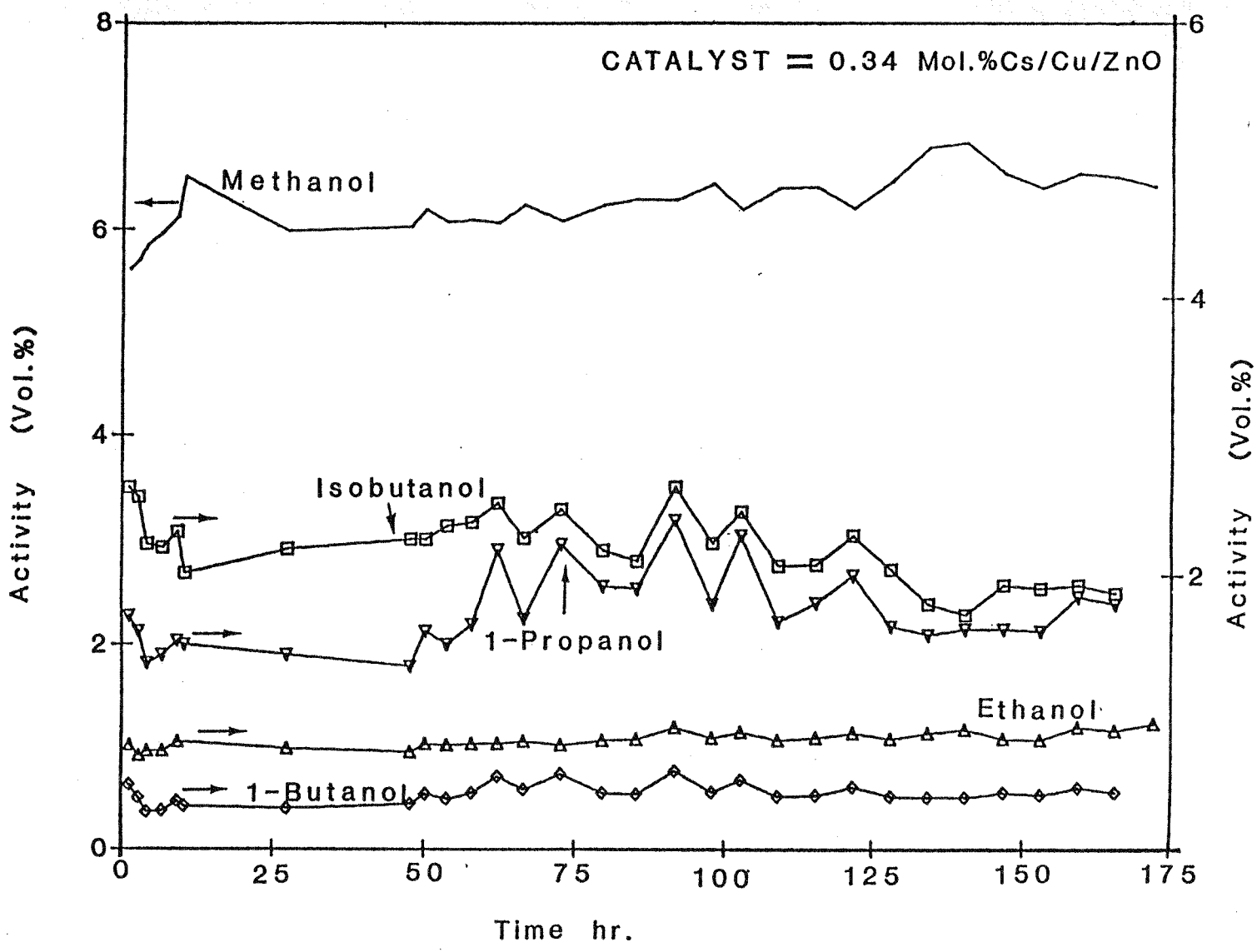

Figure 10. Effect of testing under higher alcohol synthesis conditions on the stability of the binary 0.34 mol% Cs doped Cu/ZnO catalyst for alcohol production. P = 7.6MPa; T = 310°C; Catalyst weight = 2.45 g; F = 15 l/hr; H_2/CO = 2.33.

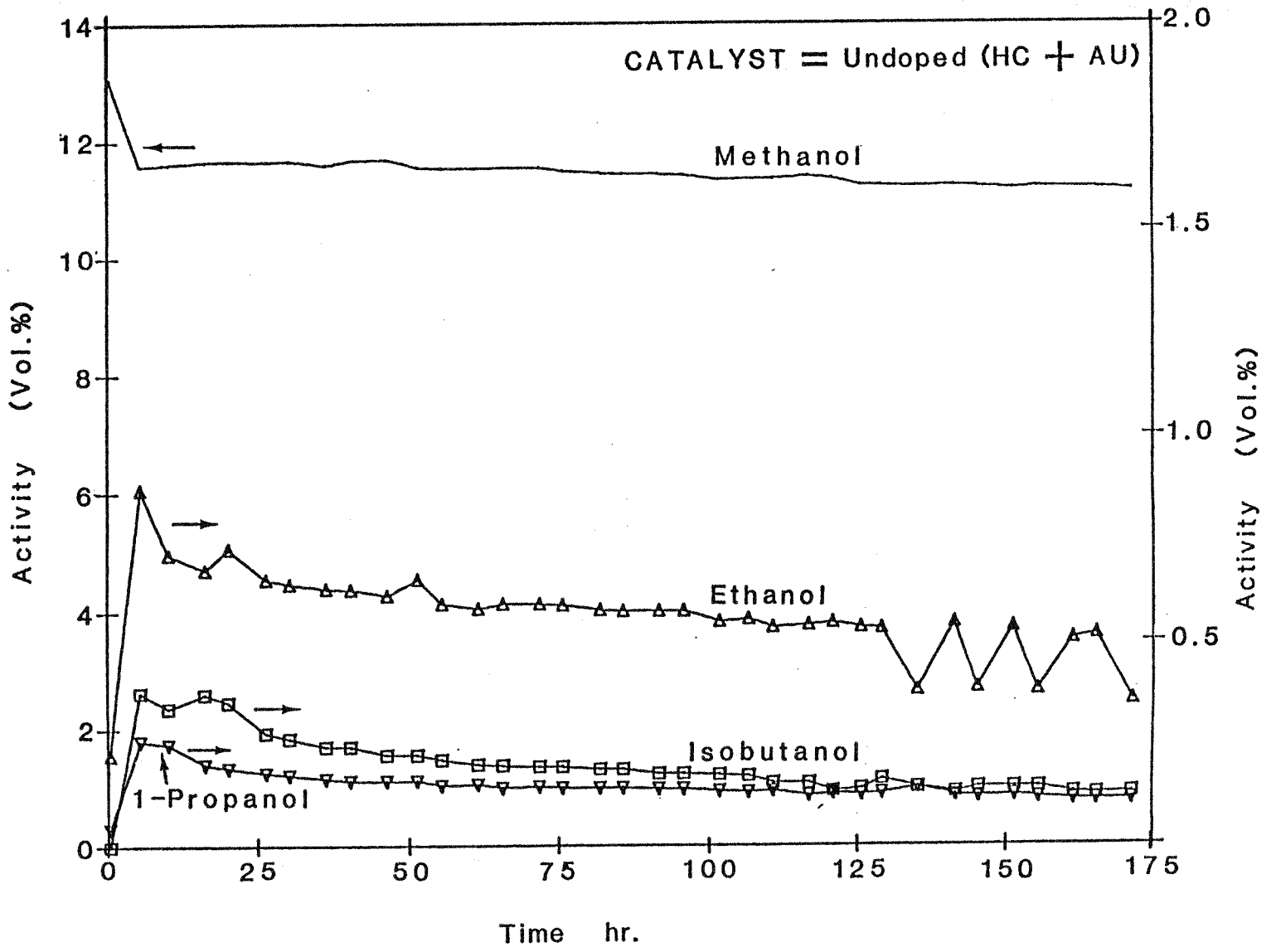

Figure 11. Effect of testing under higher alcohol synthesis conditions on the stability of the undoped (HC + AU) catalyst for alcohol production. P = 7.6MPa; T = 310°C; Catalyst weight = 2.45 g; F = 15 1/hr, H_2/CO = 2.33.

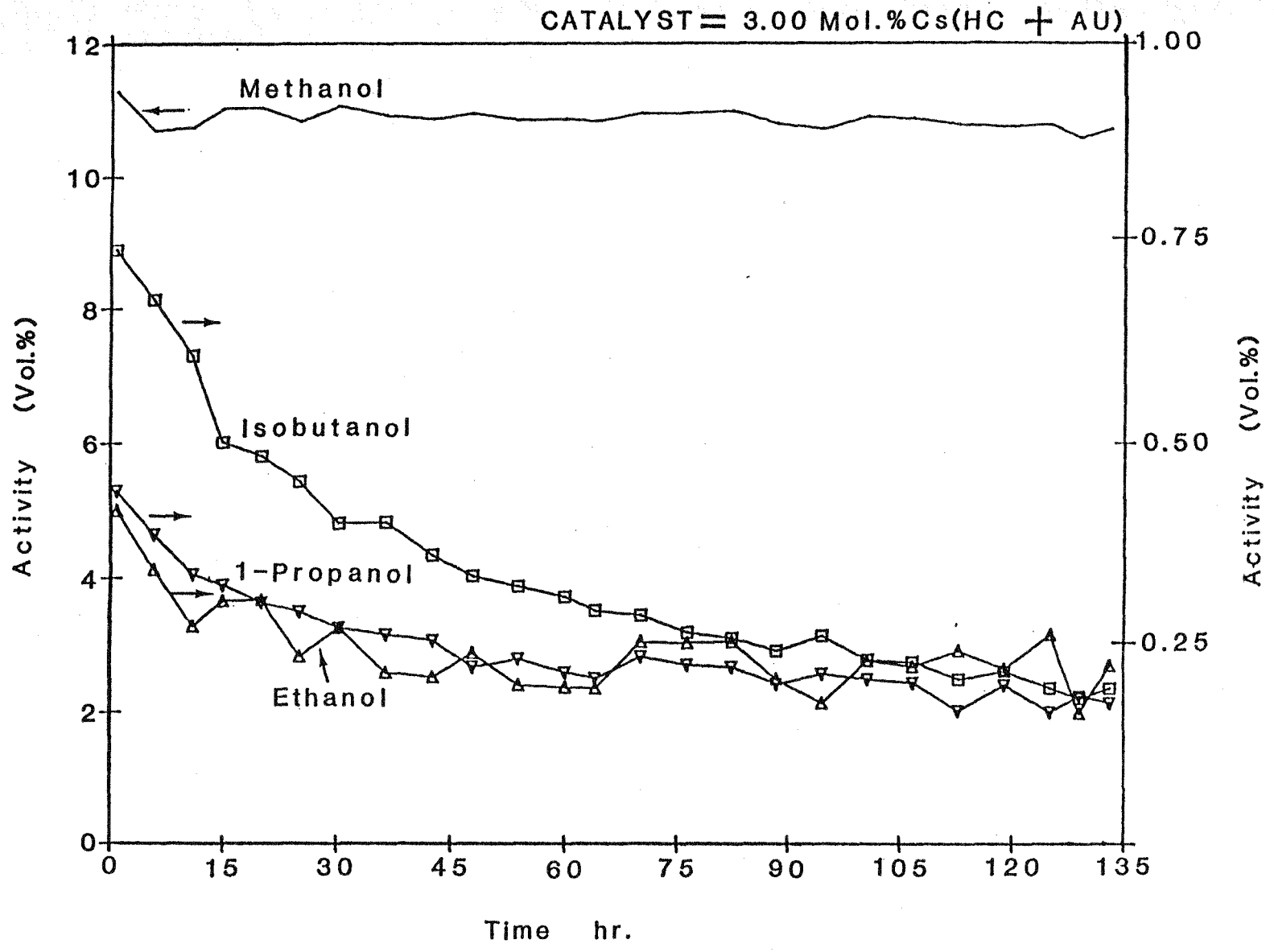

Figure 12. Effect of testing under higher alcohol synthesis conditions on the stability of the 3.00 mol% Cs doped (HC + AU) catalyst for alcohol production. P = 7.6MPa; T = 250°C; Catalyst weight = 2.45 g; F = 15 1/hr; H_2/CO = 2.33.

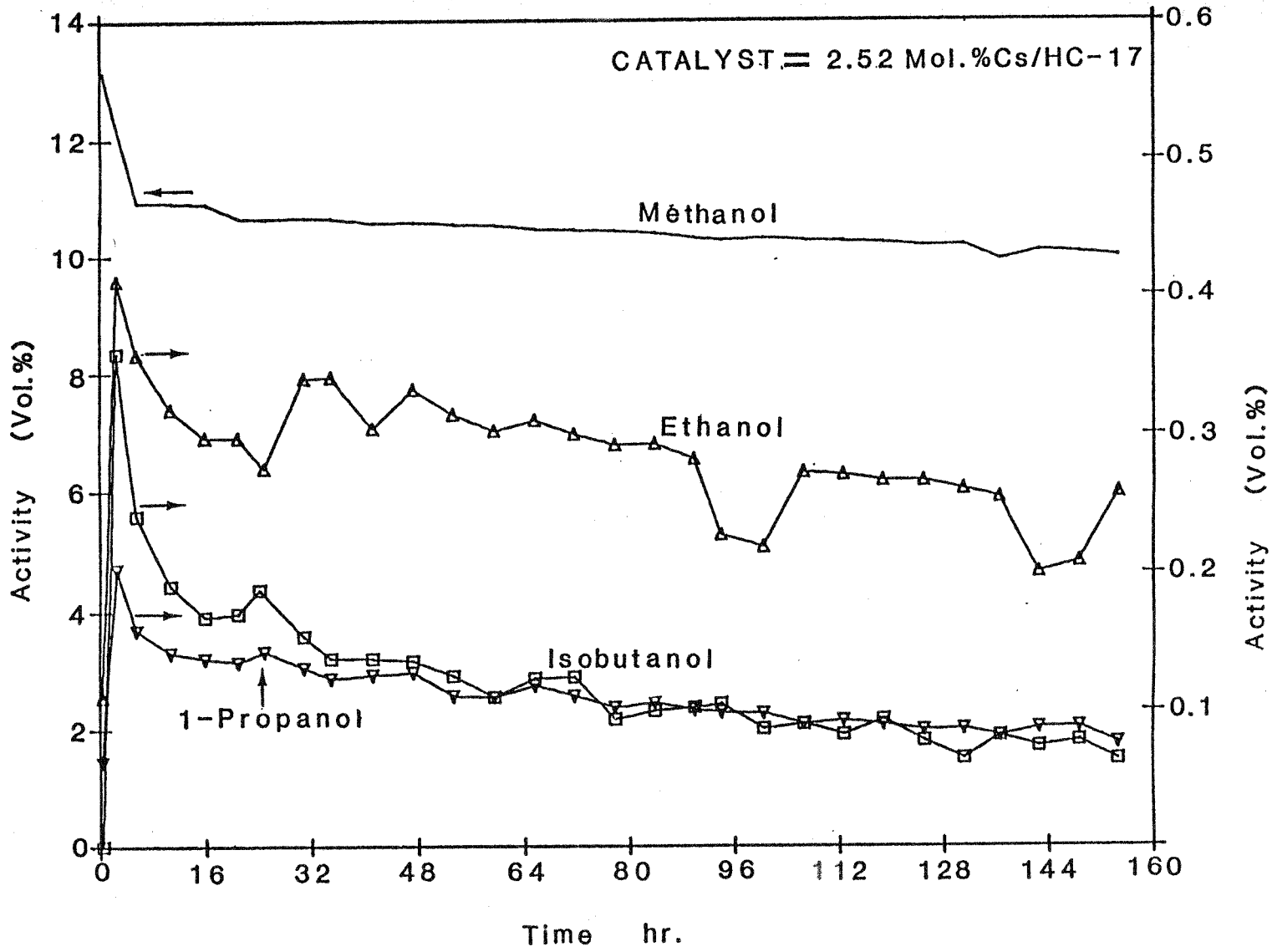

Figure 13. Effect of testing under higher alcohol synthesis conditions on the stability of the 2.52 mol% Cs HC-17 catalyst for alcohol production. P = 7.6MPa; T = 310°C; Catalyst weight = 1.5 g; F = 15 l/hr; H_2/CO = 2.33.

TABLE 8

Product yields under higher alcohol synthesis conditions of T = 310°C, P = 7.6 MPa, F = 8 l/hr and H_2/CO = 0.45. Catalyst weight = 2.45 g for all samples except HC samples where weight = 1.5 g.

		Yield (g/kg cat/hr)											
Sample	Time on Stream (hr)	CO_2	H_2O	CH_4	C_2H_6	CH_3OH	Methyl Formate	C_2H_5OH	C_3H_7OH	Iso-Butanol	Other[1] Alcohols	Methyl Acetate	Others[2]
*AU Doped with 0.34 mol% Cs	137-146	316.6	-	7.8	3.5	171.8	3.1	28.7	60.6	72.5	42.1	34.1	26.7
HC + AU Undoped	117-127	172.3	1.12	9.5	3.2	325.2	9.5	19.1	6.5	12.8	-	5.6	-
HC + AU Undoped	210-222	112.8	1.0	6.8	1.8	321.8	7.6	14.3	3.9	5.3	-	2.4	-
HC + AU Doped with 3.0 mol% Cs	78-88	150.5	1.5	6.6	1.7	283.6	5.1	7.7	9.7	18.6	-	3.0	-
HC + AU Doped with 3.0 Mol% Cs	170-182	80.5	1.1	6.6	0.7	289.5	5.3	5.2	5.3	6.9	-	1.9	-
HC-17 Doped with 0.3 mol % Cs	132-139	166.5	1.4	12.3	2.5	458.1	6.6	17.2	6.7	8.3	-	5.6	-
HC-17 Doped with 0.73 mol% Cs	142-149	183.5	2.9	11.0	2.9	521.6	7.8	15.1	4.8	6.6	-	5.6	-

[1] = 1-butanol + 2-butanol + 2-methyl-1-butanol + 1-pentanol

[2] = acetaldehyde + isobuteraldehyde + 2-butanone + methyl isobutyl ester

TABLE 8 (continued)

Product yields under higher alcohol synthesis conditions of T = 310°C, P = 7.6 MPa, F = 8 l/hr and H_2/CO = 0.45. Catalyst weight = 2.45 g for all samples except HC samples where weight = 1.5 g.

		Yield (g/kg cat/hr)											
Sample	Time on Stream (hr)	CO_2	H_2O	CH_4	C_2H_6	CH_3OH	Methyl Formate	C_2H_5OH	C_3H_7OH	Iso-Butanol	Other[1] Alcohols	Methyl Acetate	Others[2]
HC-17 Doped with 0.73 mol% Cs	236-248	108.4	2.0	11.0	1.5	487.5	8.3	9.0	1.6	1.0	-	2.4	-
HC-17 Doped with 2.52 mol% Cs	128-138	135.6	1.6	14.6	1.7	495.2	9.7	14.0	7.2	11.4	-	4.2	-
HC-17 Doped with 2.52 mol% Cs	220-232	84.80	1.3	10.2	1.2	469.4	10.2	10.4	4.4	4.6	-	2.2	-
AU* Doped with 0.34 mol% Cs	48-55	403.5	0.2	9.2	4.7	156.1	2.6	17.4	39.3	65.8	30.9	9.5	7.0

[1] = 1-butanol + 2-butanol + 2-methyl-1-butanol + 1-pentanol

[2] = acetaldehyde + isobuteraldehyde + 2-butanone + methyl isobutyl ester

table are those from the very beginning of the testing procedure. For the catalysts derived from the mixed precursor and pure hydrotalcite, doping with cesium only gave a moderate increase in isobutanol selectivity. The 0.34 mol% cesium doped binary catalyst gave relatively high activity for isobutanol formation (73 g/kg cat/hr) and maintained this high activity over the time period studied. The selectivity within the higher alcohols and other higher molecular weight products over the ternary catalyst was also substantially different than that of the binary catalyst. Only methyl-formate, methyl acetate and higher alcohols are observed, the higher alcohols consisting of ethanol, 1-propanol and isobutanol. However, this may simply be a reflection of the lower activity of these catalysts for higher alcohol synthesis rather than a sign of higher intrinsic selectivity for lower molecular weight alcohols other than methanol. Comparison of the initial activities with the long term activities over the ternary catalyst clearly shows the higher rates of deactivation for these samples - deactivation being more pronounced for the higher alcohols, 1-propanol and isobutanol.

Catalyst Deactivation

A more accurate measure of catalyst deactivation may be obtained by comparing the activities on returning to the milder reaction conditions of methanol and higher alcohol synthesis conditions and comparing the observed product yields with the initial activities. The results are summarized in Tables 9 to 13 for 5 samples. In all cases, the methanol, methyl formate and ethanol synthesis activities were greatly reduced in comparison to their initial activities under these conditions. The lowest

TABLE 9

Effect of catalyst testing at 310°C under higher alcohol synthesis conditions on the activity for methanol formation for the catalyst derived from pure Aurichalcite and subsequently doped with 0.344 mol% Cs (catalyst weight = 2.45 g).

Reaction Conditions	Time	Yield (g/kg cat/hr)							
		CO_2	H_2O	CH_4	CH_3OH	Methyl Formate	C_2H_5OH	Methyl Acetate	C_3H_7OH
T = 250°C F = 15 1/hr H_2/CO = 2.33	Before testing	8.3	0.2	4.3	587.0	5.6	1.0	-	-
T = 250°C F = 15 1/hr H_2/CO = 2.33	After testing	6.4	0.2	0.1	381.7	3.1	0.9	-	-
T = 250°C F = 8 1/hr H_2/CO = 0.45	Before testing	12.8	-	4.0	325.5	14.2	4.3	2.3	2.2
T = 250°C F = 8 1/hr H_2/CO = 0.45	After Testing	8.0	-	1.3	205.9	7.1	2.1	0.9	-

TABLE 10

Effect of catalyst testing at 310°C under higher alcohol synthesis conditions on the activity for methanol formation for the catalyst derived from the mixed precursor Hydrotalcite and Aurichalcite. (Catalyst weight = 2.45 g).

Reaction Conditions	Time	Yield (g/kg cat/hr)				
		CO_2	H_2O	CH_4	CH_3OH	Methyl Formate
T = 250° F = 15 1/hr H_2/CO = 2.33	Before Testing	8.6	0.5	3.0	309.8	0.7
T = 250° F = 15 1/hr H_2/CO = 2.33	After Testing	5.8	0.6	2.9	172.3	1.9
T = 250° F = 15 1/hr H_2/CO = 0.45	Before Testing	10.7	0.3	3.5	220.2	6.2
T = 250° F = 15 1/hr H_2/CO = 0.45	After Testing	7.9	0.2	3.3	128.1	4.2

TABLE 11

Effect of catalyst testing at 310° under higher alcohol synthesis conditions on the activity for methanol formation for the catalyst derived from the mixed precursor and subsequently doped with 3.0 mol% Cs. (Catalyst weight = 2.45 g.)

Reaction Conditions	Time	Yield (g/kg cat/hr)							
		CO_2	H_2O	CH_4	CH_3OH	Methyl Formate	C_2H_5OH	Methyl Acetate	C_3C
T = 250°C F = 15 1/hr H_2/CO = 2.33	Before Testing	10.5	0.6	4.0	802.8	3.9	0.6	-	-
T = 250°C F = 15 1/hr H_2/CO = 2.33	After Testing	6.71	-	4.5	373.7	1.7	-	-	-
T = 250°C F = 15 1/hr H_2/CO = 0.45	Before Testing	11.9	0.1	4.6	293.6	14.6	3.2	0.2	0.6
T = 250°C F = 15 1/hr H_2/CO = 0.45	After Testing	6.9	0.1	4.4	158.3	7.3	1.8		

TABLE 12

Effect of catalyst testing at 310°C under higher alcohol synthesis conditions on the activity for methanol formation for the catalyst derived from the pure precursor Hydrotalcite HC-17 and subsequently doped with 0.73 mol% Cs. (Catalyst weight = 1.5 g).

Reaction Conditions	Time	Yield (g/kg cat/hr)					
		CO_2	H_2O	CH_4	CH_3OH	Methyl Formate	C_2H_5OH
T = 250°C F = 15 1/hr H_2/CO = 2.33	Before Testing	15.0	1.0	7.0	699.7	-	-
T = 250°C F = 15 1/hr H_2/CO = 2.33	After Testing	10.3	1.1	5.5	272.2	-	-
T = 250°C F = 8.0 1/hr H_2/CO = 0.45	Before Testing	11.7	0.1	4.2	254.8	4.6	-
T = 250°C F = 8.0 1/hr H_2/CO = 0.45	After Testing	7.3	0.1	5.1	111.5	0.4	-

TABLE 13

Effect of catalyst testing at 310°C under higher alcohol synthesis conditions on the activity for methanol formation for the catalyst derived from the pure precursor Hydrotalcite HC-17 and subsequently doped with 2.52 mol% Cs. (Catalyst weight = 1.5 g).

Reaction Conditions	Time	Yield (g/kg cat/hr)					
		CO_2	H_2O	CH_4	CH_3OH	Methyl Formate	C_2H_5OH
T = 250°C F = 15 1/hr H_2/CO = 2.33	Before Testing	9.5	0.9	5.7	456.2	1.8	-
T = 250°C F = 15 1/hr H_2/CO = 2.33	After Testing	5.2	0.8	8.4	274.3	5.2	-
T = 250°C F = 8 1/hr H_2/CO = 0.45	Before Testing	12.8	0.7	8.5	445.7	15.8	-
T = 250°C F = 8 1/hr H_2/CO = 0.45	After Testing	6.58	0.2		179.8	8.06	-

relative decrease in activity occurred for the 0.34 mol% cesium doped binary catalyst. For the ternary catalysts, the ratio of the initial activity for methanol synthesis to the final activity under methanol synthesis conditions (T = 250°C, GHSV ≈ 10,000 l/kg/hr, H_2/CO = 2.33) varied from 1.7 to 2.6 as compared to 1.54 for the cesium doped binary catalyst.

Discussion

Initial testing results reveal a dramatic difference in activities, selectivities, and stabilities of the binary Cu/ZnO catalyst and the ternary Cu/Zn/Al catalysts. Under higher alcohol synthesis conditions, the binary catalyst exhibited both high selectivity for higher alcohols, in particular 1-propanol and isobutanol, and high stability. However, the catalyst did show some deactivation as a result of testing under these conditions as shown in Table 9. In the case of catalysts derived both from the mixed precursor and the pure hydrotalcite precursor, a lower level of higher alcohol synthesis was observed, accompanied with more rapid deactivation with time. However, these catalysts did show very high methanol synthesis activities, as shown in Figure 8 for HC-17 and in Table 6 for the 3.0 mol% Cs-doped mixed precursor (HC + AU). Thus, the ternary catalysts as prepared in this study, even though not being very selective for higher alcohol synthesis, are exceptionally active alcohol synthesis catalysts. The undoped HC-17 is the most active methanol synthesis catalyst yet tested in this laboratory in the absence of CO_2 and water, and the results of Figure 8 indicate that this sample would be an extremely active catalyst in the presence of CO_2.

One of the most important features of the present study is the differing effects of cesium-doping on the catalytic activity for catalysts derived from the pure precursor, hydrotalcite, as compared to the aurichalcite or mixed precursor derived catalysts. In order to attempt to explain these differences, some features of the tested catalysts and the effects of cesium doping on morphology and activity must be considered.

(i) The initial hydrotalcite precursor as prepared by coprecipitation was sky-blue in color. Upon calcination, the color changed to a deep-green, but upon rehydration the color did not go back to the initial blue color but rather was dark gray, even though the XRD analysis showed that the hydrotalcite-like structure had been regenerated. This indicates that at least some of the ion positions are not the same in the reconstituted hydrotalcite, and in particular, that some of the Cu^{2+} ions (which are probably the origin of the blue color) are not in the original lattice locations.

(ii) In contrast to the binary catalyst where the oxide form of the catalyst is doped, doping the catalysts derived from the mixed precursor or the pure hydrotalcite precursor involved doping the hydroxycarbonate form of the catalyst. These latter catalysts then have to be recalcined to give the oxide form.

(iii) The TEM studies showed that the catalysts existed in a platelet form for both the hydroxycarbonate and oxide forms and that the platelets for both were of similar shape and size. This surprising result suggests that the interconversion from one form to the other occurs within the same particle, i.e. is very localized and thus the overall morphology of one phase may have a large influence on the other, e.g. the nature of the micropore structure might be similar. The XRD diffraction analysis, c.f. Table 5

further showed that the particles are larger for the hydrotalcite formed after rehydration and the TEM studies showed that the reformed platelets may be larger than the original ones. These changes may have a dramatic effect on the activity of the final catalyst. It should be further pointed out that there are some important morphological features not detected by the TEM or XRD studies used here. These may include smaller or larger micropore structures with accompanying large changes in surface area of the active catalyst and thus catalytic activity.

(iv) Even though the initial effect of doping the pure phase hydrotalcite is loss of activity, c.f. Table 6, increasing the level of cesium doping gives rise to a promotion effect on both methanol and methyl formate synthesis as shown in Table 7. This indicates that cesium itself is not a poison for the reaction, as the activity should decrease further or remain constant, but that the initial deactivation is apparently brought about by the doping process, i.e. the reconstitution of the hydrotalcite structure. In the case of the mixed precursor derived catalyst, the undoped tested catalyst was not obtained from clacination of the precipitate directly as was HC-17, but rather was obtained from a rehydrated-recalcined sample so that we are starting from a deactivated catalyst and the effect of cesium doping is now just a promotional effect.

The doping process adopted clearly leads to a deactivation in methanol synthesis; however, the effect on higher alcohol synthesis may even be greater, thus reducing the catalyst selectivity for the higher alcohol formation. Therefore, initial efforts during the next quarter will be directed towards doping with cesium without deactivating the catalyst in

the process.

The more rapid deactivation of the ternary catalysts may be due to the presence of some residual acidity on the catalyst surface leading to coking or due to a more rapid loss of surface area for these samples. The acidic nature of these catalysts is evidenced by the detection of traces of dimethyl ether and ethylene in the products under higher alcohol synthesis conditions. Higher doping levels with the basic cesium may be beneficial not only in promoting higher alcohols but in neutralizing the acidity (and thus preventing deactivation). This, in fact, is born out by the results since dimethyl ether and ethylene were detected for the 0.73 mol% hydrotalcite-derived samples (1.3 and 0.8 g/kg cat/hr, respectively) but were absent from the 2.52 mol% Cs-doped sample, which also showed the least amount of deactivation (Table 7). From Tables 11 and 12, it is further found that the ratio of the initial and final methanol synthesis rates at T = 250°C, GHSV = 10,000 l/kg/hr, and H_2/CO = 2.33 were 2.57 for the 0.73 mol% sample, but only 1.66 for the 2.5 mol% doped sample very close to that for the binary sample.

Summary

1. Preparation of a single-phase hydrotalcite-like precursor has been successfully accomplished.
2. TEM studies have shown that both the precursor and oxide form exist in a single platelet morphology.
3. Rehydration of the calcined oxide form of the catalyst leads to reconstitution of the hydrotalcite-like structure.
4. Catalysts obtained by calcination of the hydrotalcite-like precursor are extremely active methanol synthesis catalysts.

5. Doping with cesium leads to initial deactivation that is partially recovered by doping at higher levels.

6. Initial studies showed that the catalyst derived from the mixed phase precursors (HC + AU) or pure phase hydrotalcite exhibit low selectivity for higher alcohol synthesis while still being active methanol synthesis catalysts.

7. Deactivation is least over the binary samples, however, higher loading of cesium in the ternary catalyst led to a marked increase in catalyst stability under higher alcohol synthesis conditions.

Future Work

1. The activity of the undoped HC-17 and HC-18 catalyst will be determined under higher alcohol synthesis conditions.

2. Testing of HC-19 and HC-20 under methanol synthesis conditions to determine initial activities of these samples.

3. HC-18 (same preparation as HC-17) will be doped with cesium while avoiding the rehydration and subsequent reconstitution of the hydroxycarbonate form of the catalyst. This will be accomplished by

(i) doping the original precipitate, and

(ii) doping the calcined catalyst under dry nitrogen in a non-aqueous solvent.

If Cs-doping without deactivation can be accomplished, then the catalysts will be extensively tested under higher alcohol synthesis conditions.

4. Doping with higher levels of cesium to determine the effect on higher alcohol synthesis selectivity and catalyst stability.

5. Extensive characterization of all catalysts tested, and for all stages of catalyst preparation, using XRD, XPS, TEM, surface area measurements, porosity studies and, in the light of the color changes observed, U.V. visible diffuse reflectance spectroscopy.

References

1. Busetto, C., Del Piero, G., Manara, G., Trifiro, F., and Vaccari, A., J. Catal., 85, 260 (1984).

2. Anderson, J. R., "Structure of Metallic Catalysts," Academic Press, NY, 366 (1975).

3. Herman, R. G., Simmons, G. W., and Klier, K., Proc. 7th Intern. Congr. Catal., ed. by T. Seiyama and K. Tanabe, Elsevier, Amsterdam, 475 (1981).

4. Klier, K., Chatikavanij, V., Herman, R. G., and Simmons, G. W., J. Catal., 74, 343 (1982).